

REPRESENTATIONS OF COULOMB FRICTION FOR DYNAMIC ANALYSIS

NASER MOSTAGHEL* AND TODD DAVIS†

Department of Civil Engineering, University of Toledo, Toledo, OH 43606-3390, U.S.A.

SUMMARY

In many engineering problems involving friction, the friction is treated as Coulomb friction, where the magnitude of the friction force is constant but its direction is always opposite to that of the sliding velocity. In dynamic problems, the direction of the sliding velocity can change quite often. The many changes of the velocity direction cause many discontinuities in the friction force, complicating the process of evaluating the response of systems involving friction. In this paper, it is shown that the discontinuous Coulomb friction force can be represented by at least four different continuous functions. Each of these functions involves one constant that controls the level of accuracy of that function's representation of the friction force. The accuracy of the various representations is verified by comparing the response of a single degree freedom system, obtained through numerical solutions utilizing these representations, with an exact analytical solution. © 1997 by John Wiley & Sons, Ltd.

KEY WORDS: friction; Coulomb; dynamic; sliding; stick slip

1. INTRODUCTION

Friction is present in many engineering problems. It is an integral part of a number of seismic isolation systems. Detailed overviews of these system have been presented by Kelly¹ and Buckle and Mays.² In the systems involving friction, the friction force has been idealized as Coulomb where, as long as there is motion, the magnitude of friction force is constant and its direction is opposite to that of the sliding velocity. As a result, whenever the sliding velocity crosses zero, the friction force makes a sudden change in direction. This sudden change in the direction of the friction force makes the system extremely non-linear and the solution process highly complicated. Den Hartog³ has given an analytical solution for a single degree of freedom system under harmonic excitations. Levitan [4] used a Fourier Series representation of Coulomb friction force and treated the continuous motion of a system under forced oscillation. For seismic loadings, the excitations are highly irregular and the problem has to be treated numerically. To linearize the problem for small friction coefficients, the Coulomb friction has been approximately represented by an equivalent viscous damping by a number of investigators.^{5–8} Fictitious spring, rigid plastic, and hysteretic models involving experimentally evaluated parameters have also been used to model the effects of Coulomb friction.^{9–12} The hysteretic model provides the most satisfactory representation. However, additional non-linear differential equations with associated hysteretic parameters have to be incorporated into the governing system of equations.

Based on the fact that in each sliding and non-sliding phase the system's behaviour is linear, two-phase models have been proposed, criteria for start and end times of sliding and non-sliding phases have been formulated, and solutions for special cases have been implemented by a number of researchers.^{13–21} Although the two-phase model works well with common types of ground motions, for very high-frequency

*Professor

†Graduate Student

base motions that one may encounter in the isolation of equipment, unless the integration steps are extremely small, the cumulative errors may become too large. The transition boundaries of sliding and non-sliding phases are characterized by the zero crossings of the sliding velocity. No matter how small the integration steps, it is not possible to identify the exact times of zero crossing for the sliding velocity numerically. Also if there are many sliding devices incorporated into a structure, keeping track of all the phases for all the sliding devices will simply become too cumbersome. Here it is proposed to replace the discontinuous friction-force sliding-velocity relation with a continuous function. This continuous function representation of the Coulomb friction force completely eliminates the need to keep track of stick-slip phases and their transitions. As will be seen, the continuous function can be selected to be arbitrarily close to the exact discontinuous friction force. Four continuous functions are considered for this study. Undoubtedly others with similar characteristics may be formulated. One of the functions is used for detailed investigation with applications to systems subjected to harmonic excitations.

2. ANALYSIS

The Coulomb friction force is defined by

$$F_f = -\mu mg \operatorname{Sgn}[\dot{u}(t)] \quad (1)$$

where F_f denotes the friction force, m is the mass of the structure, g is the gravitational acceleration, and $\dot{u}(t)$ is the sliding velocity as a function of time. Here, μ , the friction coefficient, is assumed to be constant. However, a friction coefficient which is a function of sliding velocity (as in the case of teflon-stainless steel interface) can be incorporated in equation (1). The sign of the sliding velocity is represented by the Signum function,

$$\operatorname{Sgn}[\dot{u}(t)] = \begin{cases} +1 & \text{for } \dot{u}(t) > 0 \\ 0 & \text{for } \dot{u}(t) = 0 \\ -1 & \text{for } \dot{u}(t) < 0 \end{cases} \quad (2)$$

To provide an application context, for simplicity we consider a rigid structure supported on an isolation system, shown in Figure 1. The isolation system involves restoring force, viscous damping force and friction force. A mechanical model of the system is shown in Figure 2. This kind of isolation system can be realized in

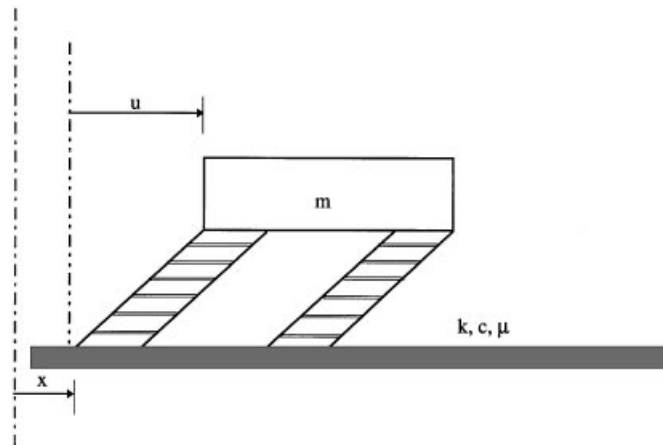


Figure 1. A rigid structure supported on a base isolation system

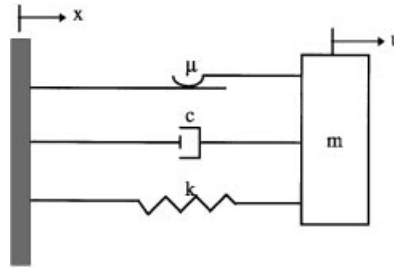


Figure 2. Schematic representation of a base isolated structure

isolation devices proposed by a number of investigators. The equilibrium equation governing the motion of this type of system in sliding phases is given by

$$m\ddot{u} + c\dot{u} + ku + m\mu g \operatorname{Sgn}[\dot{u}] = -m\ddot{x} \quad (3)$$

where \ddot{x} is the base acceleration, and u is the response displacement. In non-sliding phases $\dot{u} = \ddot{u} = 0$, $u = \text{constant}$, and $|\omega^2 u + \ddot{x}| < \mu g$. At transition from a non-sliding phase to a sliding phase, $|\omega^2 u + \ddot{x}| = \mu g$. It should be noted that, even though equation (1) is only valid during sliding phases, since the relative displacement u remains constant during each non-sliding phase, equation (3) defines u for both sliding and non-sliding phases. The conventional form of equation (3) is

$$\ddot{u} + 2\zeta\omega\dot{u} + \omega^2 u + \mu g \operatorname{Sgn}[\dot{u}] = -\ddot{x} \quad (4)$$

where $\omega = \sqrt{k/m}$ is the natural frequency and $\zeta = c/2\omega m$ is the damping ratio. If the base acceleration is defined by

$$\ddot{x} = a \sin \Omega t \quad (5)$$

then the following substitutions:

$$\tau = \omega t, \quad \beta = \Omega/\omega, \quad \delta = ma/k, \quad u = v\delta \quad \text{and} \quad \alpha = \mu g/a$$

into equation (4) yield

$$\ddot{v} + 2\zeta\dot{v} + v + \alpha \operatorname{Sgn}[\dot{v}] = \sin \beta\tau \quad (6)$$

The analytical solution to equation (6) has been provided by Den Hartog [3]. This analytical solution will be used to validate the various representations of the Coulomb friction force which will be proposed here.

The Signum function defined in equation (2) can be represented by any of the following four continuous functions to any desired level of accuracy:

$$\begin{aligned} f_1(\alpha_1, \dot{u}) &= \operatorname{Erf}(\alpha_1 \dot{u}) \\ f_2(\alpha_2, \dot{u}) &= \operatorname{Tanh}(\alpha_2 \dot{u}) \\ f_3(\alpha_3, \dot{u}) &= (2/\pi) \operatorname{ArcTan}(\alpha_3 \dot{u}) \\ f_4(\alpha_4, \dot{u}) &= \alpha_4 \dot{u} / (1 + \alpha_4 |\dot{u}|) \end{aligned} \quad (7)$$

A comparison of variations of these functions with the sliding velocity, \dot{u} for the factor $\alpha_i = 10$ ($i = 1, 2, 3, 4$), is given in Figure 3. The factors α_i 's are all positive. Their values dictate the desired level of accuracy in their

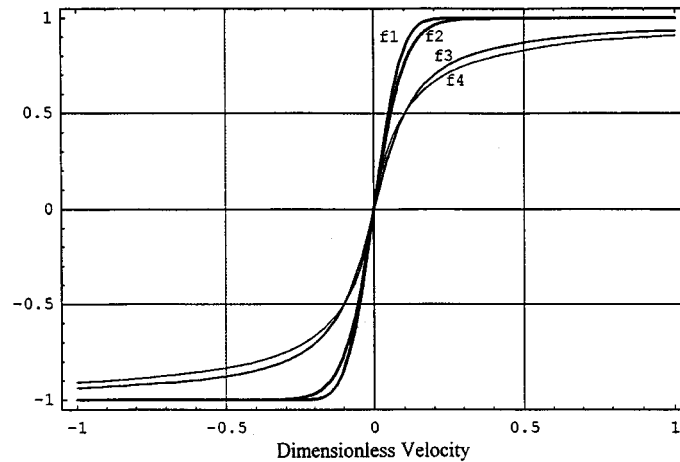


Figure 3. Comparisons of the four representations of the signum function ($\alpha_i = 10$, $i = 1, 2, 3, 4$)

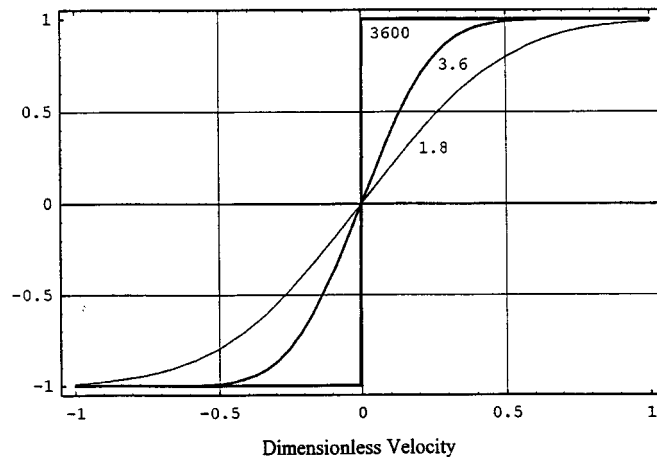


Figure 4. Representation of the signum function by $f_1(\alpha_1 = 1.8, 3.6, 3600)$

respective representations of the Signum function. For example, if the unit of velocity is in mm/s, then an $\alpha_1 = 3.6$ implies that for magnitudes of velocities larger than 1 mm/s

$$f_1(\alpha_1, \dot{u}) = \text{Erf}(3.6 \dot{u}) = \pm 1 \quad (8)$$

with six decimal accuracy. Therefore, if an $\alpha_1 = 3600$ is used, then for magnitudes of sliding velocities larger than 10^{-3} mm/s, the value of the error function will be ± 1 with six decimal accuracy. This implies that the function $f_1(\dot{u})$ changes continuously from -1 to $+1$ when the velocity goes from -10^{-3} to $+10^{-3}$ mm/s. From a practical point of view, these velocities are in the neighbourhood of zero and the Signum function as defined in relations (2) can be approximately represented by the continuous function $f_1(\dot{u})$. Figure 4 shows the variations of $f_1(\dot{u})$ with the sliding velocity for the factor $\alpha_1 = 1.8$, $\alpha_1 = 3.6$, and $\alpha_1 = 3600$. Similar arguments apply to the other three functions in equation (7) except that different values of α_i 's have to be used to gain the equivalent levels of accuracy. Considering these results, it can be concluded that for sufficiently large α_i for practical applications,

$$\text{Sgn}[\dot{u}] = f_i[\alpha_i, \dot{u}] \quad (9)$$

Thus for sufficiently large α_i , the friction force in equation (1) may be represented by

$$F_f(t) = -\mu m g f_i[\alpha_i, \dot{u}(t)], \quad i = 1, 2, 3, 4 \quad (10)$$

and the Signum function in equations (3), (4) and (6) can be replaced by f_i , $i = 1, 2, 3, 4$. It should be noted that the representations of the friction force as defined by equation (10) are only valid when the mass is in a sliding phase. In non-sliding phases, the friction force is undefined and its magnitude is less than that given by equation (10).

3. VERIFICATION

Before using the proposed representations of the friction force to solve the general base excitation problem of equation (4), we will use them to solve the problem of harmonic base excitations represented by equation (6). Den Hartog's analytical solution [3] will be used to validate the quality of the proposed representations. Table I presents the non-dimensionalized maximum displacement responses (for the case of $\beta = 1$) as obtained by the analytical solution and by the various representations of the Coulomb friction force for $\alpha = \mu g/a = 0.40$ and $\alpha = \mu g/a = 0.50$, a damping of $\zeta = 2$ and 5%, and for the factor $\alpha_i = 10, 100$, and 1000. As can be observed from this table in all cases when the factor α_i is of the order of 100 or larger, the maximum difference with the analytical solution is less than 1%.

Now that the numerical solutions for various representations of the Coulomb friction force have been validated by comparisons with Den Hartog's analytical solution, we can use these representations in the dynamic analysis of any system involving friction.

As examples, responses to harmonic excitations for two systems, which are identical except for the value of their friction coefficients, are presented in Figures 5–8. These figures are for the case of $\zeta = 2\%$, $\beta = 0.4$ and $\alpha = \mu g/a = 0.40$, and for the case of $\zeta = 2\%$, $\beta = 0.4$ and $\alpha = \mu g/a = 0.90$. Figures 5 and 7, which show the variations of the dimensionless displacement and velocity responses, clearly display the stick and the slip regions, and comparisons of these figures also show that, as expected, the duration of the non-sliding phases increases with the increase of the friction force. Figures 6 and 8 show the variations of the dimensionless total acceleration with displacement. The sharpness of the angles at the corners of the loops attest to the quality of the proposed representations for the Coulomb friction.

Table I. Comparisons of various representations with Den Hartog solution

ζ $\alpha = \mu g/a$	0.02		0.05		factor α_i
	0.4	0.5	0.4	0.5	
Den Hartog	12.2824	9.1029	4.9274	3.6589	
f_1	12.2359	9.0611	4.9058	3.6327	10
	12.2354	9.0598	4.9052	3.6313	100
	12.2352	9.0597	4.9052	3.6313	1000
f_2	12.2358	9.0612	4.9062	3.6335	10
	12.2353	9.0601	4.9052	3.6313	100
	12.2352	9.0599	4.9052	3.6313	1000
f_3	12.3402	9.2348	5.0064	3.7978	10
	12.2459	9.0781	4.9157	3.6489	100
	12.2363	9.0621	4.9063	3.6331	1000
f_4	12.395	9.3229	5.0548	3.8722	10
	12.2518	9.0879	4.9214	3.6585	100
	12.2369	9.0629	4.9068	3.6341	1000

All the integrations of the differential equation for the above examples were performed via the Runge–kutta method imbedded in Mathematica.²² These figures clearly show the effectiveness of isolation systems involving friction in limiting the system response.

4. DISCUSSION AND CONCLUSIONS

The results presented in Figures 5–8 are based on using the function f_4 with an $\alpha_4 = 1000$ to represent the signum function. This function is used because for the same levels of accuracy, the integration time is shorter for this function as compared to functions f_1 and f_2 and is about the same as for function f_3 . In place of the integer 1 in the denominator of the expression for f_4 in equation (7), one may use a number less than unity. However, it can be shown that the effects of any number in place of this integer can be equivalently represented by α_4 .

Considering the results presented in Table I and Figures 5–8, where the levels of μg range from 40 to 90% of the peak excitation acceleration, it can be concluded that the proposed approximation for the friction force

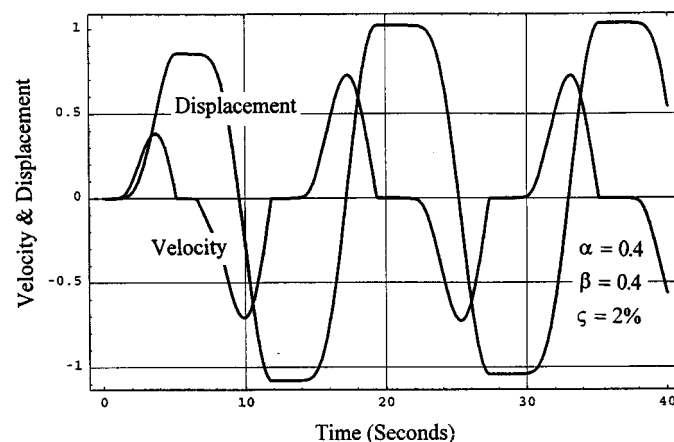


Figure 5. Time-histories of non-dimensional velocity and displacement

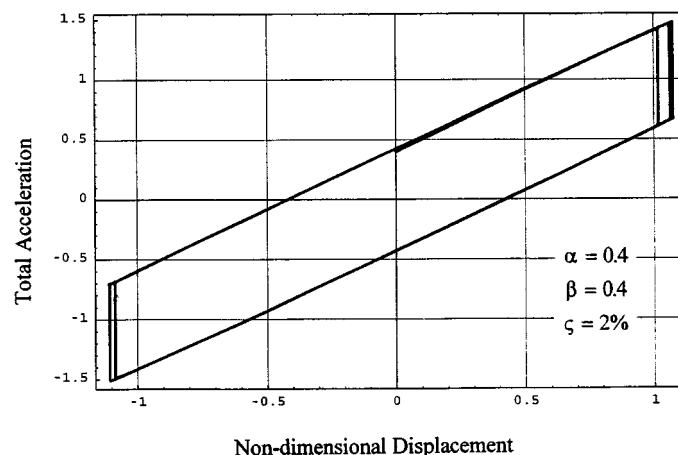


Figure 6. Variations of force with displacement

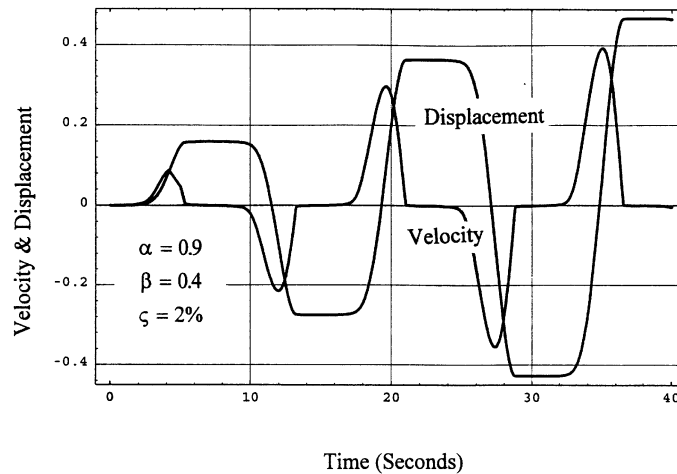


Figure 7. Time-histories of non-dimensional velocity and displacement

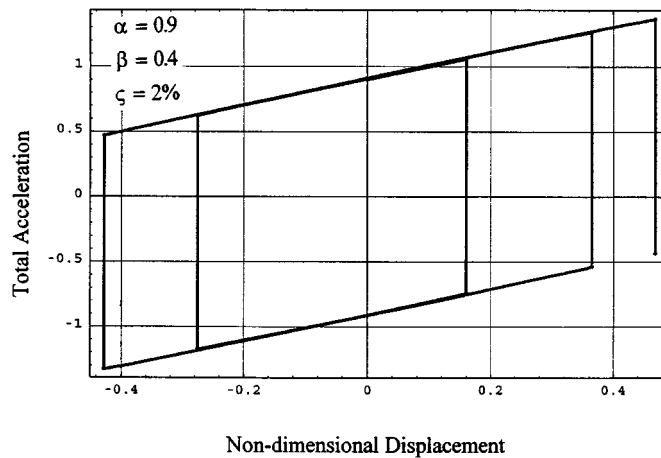


Figure 8. Variations of force with displacement

is applicable for small as well as large values of the friction coefficient. Of course the level of approximation can be improved by using larger values for α_i . It is noted that equation (10) is valid even if the friction coefficient is a function of the sliding velocity or a function of time.

ACKNOWLEDGEMENTS

Thanks are given to Dr. Douglas L. Oliver of the Mechanical, Industrial and Manufacturing Engineering Department at the University of Toledo for helpful discussions.

REFERENCES

1. J. M. Kelly, 'Aseismic base isolation: review and bibliography', *Soil dyn. earthquake eng.*, **5**(3), 202–217 (1986).
2. I. C. Buckle and R. L. Mays, 'Seismic isolation: history, application and performance—a world overview', *Earthquake spectra* **6**, 161–202 (1990).
3. J. P. Den Hartog, 'Forced vibrations with combined coulomb and viscous friction'. *Trans. Am. soc. mech. eng. (ASME)* **53**, 107–115 (1931).

4. E. S. Levitan, 'Forced oscillation of a spring-mass having combined coulomb and viscous damping', *J. acoust. soc. Am.* **32**, 1265–1269 (1960).
5. J. M. Kelly and K. E. Beucke, 'A friction damped base isolation system with fail-safe characteristics', *Earthquake eng. struct. dyn.* **11**, 33–56 (1983).
6. K. E. Beucke and J. M. Kelly, 'Equivalent linearizations for practical hysteretic systems', *International J. non-linear mech.* **23**, 211–238 (1985).
7. L. Su, G. Ahmadi, 'Response of friction base isolation systems to horizontal-vertical random earthquake excitations', *Probab. eng. mech.* **3**(1), 12–21 (1988).
8. L. Su, G. Ahmadi, 'Probabilistic responses of base-isolated structures to El Centro 1940 and Mexico City 1985 earthquakes', *Eng. struct.* **14**(4), 217–230 (1992).
9. Y. B. Yang, T. Y. Lee and I. C. Tsai, 'Response of multi-degree-of-freedom structures with sliding supports', *Earthquake eng. struct. dyn.* **19**, 739–752 (1990).
10. C. E. Grigorian and E. P. Popov, 'Slotted Bolted Connections for Energy Dissipation', in Proc. ATC-17-1 seminar on base isolation and passive energy dissipation, Vol. 3, San Francisco, 1993, pp. 545–556.
11. M. Constantinou, A. Mokha and A. M. Reinhorn, 'Teflon bearing in base isolation, part II: modeling', *J. struct. eng.* **116**, 455–474 (1990).
12. G. Ahmadi, F. G. Fan and M. N. Noori, 'A thermodynamically consistent quasi-linear model for hysteretic materials', *Report No. MAE-223*, Clarkson University, January 1991.
13. G. Ahmadi and L. Su, 'Response of a friction base isolator to random earthquake excitations', in *Seismic Engineering, Recent Advances in Design Analysis, Testing, and Qualification Methods*, ASTM, PVP-V.127, 1987, pp. 399–404.
14. L. Su, G. Ahmadi and I. G. Tadjbakhsh, 'A comparative study by performances of various base isolation systems, part I: shear beam structures', *Earthquake eng. struct. dyn.*, **18**, 11–32 (1989).
15. L. Su, G. Ahmadi and I. G. Tadjbakhsh, 'A comparative study of performances of various base isolation systems, part II: sensitivity analysis', *Earthquake eng. struct. dyn.* **19**, 21–33 (1990).
16. S. R. Malushte and M. P. Singh, 'A study of seismic response characteristics of structures with friction damping', *Earthquake eng. struct. dyn.* **18**, 767–783 (1989).
17. N. Mostaghel, M. Hejazi and J. Tanbakuchi, 'Response of sliding structures to harmonic support motion', *Earthquake eng. struct. dyn.* **11**, 355–366 (1983).
18. N. Mostaghel and J. Tanbakuchi, 'Response of sliding structures to earthquake support motion', *Earthquake eng. struct. dyn.* **11**, 729–748 (1983).
19. N. Mostaghel and M. Khodaverdian, 'Dynamics of resilient-friction base isolator (R-FBI)', *Earthquake eng. struct. dyn.* **15**, 379–390 (1987).
20. N. Mostaghel and M. Khodaverdian, 'Seismic response of structures supported on R-FBI system', *Earthquake eng. struct. dyn.* **16**, 839–854 (1988).
21. A. G. Hernried and K. M. Lei, 'Parametric studies on the response of equipment in resilient-friction base isolated structures subjected to ground motion', *Int. j. eng. struct.* **15**, 349–357 (1993).
22. S. Wolfram, 'Mathematica, A System for Doing Mathematics by Computer', Addison-Wesley, Reading, MA, 1991.